



Contents lists available at ScienceDirect



# Catalysis Today

journal homepage: [www.elsevier.com/locate/cattod](http://www.elsevier.com/locate/cattod)

## Fischer Tropsch synthesis using cobalt based carbon catalysts

Sarwat Iqbal<sup>a</sup>, Thomas E. Davies<sup>b</sup>, David J. Morgan<sup>a</sup>, Khalid Karim<sup>c</sup>, James S. Hayward<sup>a</sup>, Jonathan K. Bartley<sup>a</sup>, Stuart H. Taylor<sup>a</sup>, Graham J. Hutchings<sup>a,\*</sup>

<sup>a</sup> Cardiff Catalysis Institute, School of Chemistry, Cardiff University, Main Building, Park Place, Cardiff CF10 3AT, UK

<sup>b</sup> Stephenson Institute for Renewable Energy, Chemistry Department, The University of Liverpool, Crown Street, Liverpool L69 7ZD, UK

<sup>c</sup> SABIC T&I, P.O Box 42503, Riyadh 11551, Saudi Arabia

### ARTICLE INFO

#### Article history:

Received 3 August 2015

Received in revised form

10 September 2015

Accepted 11 September 2015

Available online xxx

#### Keywords:

Fischer Tropsch synthesis

Syngas

Carbon support

Cobalt

Cobalt manganese catalysts

### ABSTRACT

The catalytic activity of a series of carbon-supported cobalt manganese oxide ( $\text{CoMnO}_x$ ) catalysts was investigated for the Fischer Tropsch synthesis reaction. The catalysts were compared with an unsupported  $\text{CoMnO}_x$  catalyst under the same reaction conditions, and it was shown that the use of an activated carbon support increased both the catalyst activity and the selectivity to  $\text{C}_{2+}$  hydrocarbons, whilst lowering the selectivity to  $\text{CH}_4$  and  $\text{CO}_2$ . Additionally, the effects of varying heat treatment temperatures and increasing the precursor ageing times were also investigated. Increasing the heat treatment temperature of the catalyst precursor between 300 and 500 °C led to an increase in activity, as well as an increase in selectivity to  $\text{C}_{2+}$  hydrocarbons, but it also increased the selectivity to  $\text{CO}_2$ . At 600 °C there was a marked decrease in activity, and the main product was  $\text{C}_{5+}$  hydrocarbons. Ageing the initial precipitate led to a decrease in activity and also decreased the selectivity towards hydrocarbons.

© 2015 Elsevier B.V. All rights reserved.

## 1. Introduction

Fischer Tropsch synthesis (FTS) is valuable for the production of clean liquid fuels from syngas ( $\text{CO} + \text{H}_2$ ). The product distribution in FTS is, however, typically very broad and a major part of the extensive current research is focussed on controlling the selectivity to the desired products. Fe, Co, and Ru are active catalysts for FTS, but only Fe and Co are used extensively. Although ruthenium exhibits excellent activity for this reaction, its limited availability and cost prohibits its use on an industrial scale. Iron based catalysts have been shown to be active for the formation of hydrocarbons at higher reaction temperatures, but suffer from complex phase formation and deactivation by water. Cobalt catalysts are active at lower temperatures than Fe and tend to produce light hydrocarbons, particularly when promoted with manganese oxide. A range of studies have been published on  $\text{CoMnO}_x$  catalysts for the synthesis of light hydrocarbons, and they demonstrate lower selectivity to methane [1–4]. It has been observed that Co in combination with manganese oxide can produce high yields of alkenes with increasing CO conversion, whereas this is not observed with cobalt only catalysts [5]. The use of partially reducible oxides such as  $\text{MnO}_2$  and  $\text{TiO}_2$  [4] has been shown to improve the selectivity towards

light alkenes in FTS using cobalt as the active metal component. There are reports showing the structure–performance relationship of  $\text{CoMnO}_x$  catalysts which supports the hypothesis that it is necessary for Co and Mn to be in close proximity to observe the enhanced catalytic performance [6].

It is well-established that the catalytic activity depends on the number of surface metal sites available for reaction. A common method of increasing the dispersion and stability of metal is supporting the particles on a stable metal oxide, such as  $\text{Al}_2\text{O}_3$  or  $\text{SiO}_2$ . However, it has been observed that the strong metal–support interaction can lead to the formation of undesirable phases such as  $\text{CoAl}_2\text{O}_4$ , and these mixed oxides are believed to be a cause of deactivation that is generally observed with these catalysts. The utilization of inert supports can present an alternative approach, in this way it might be possible to improve the dispersion and stability of the active metal sites without risking the formation of the inactive mixed metal oxide. Materials based on activated carbon have been reported to be promising supports because they are relatively chemically inert [7–9]. Carbon provides a stable platform for the deposition of the active species [10] and carbon has been shown to enable the reduction of metal oxides in an inert atmosphere, as a result of auto-reduction [11]. To date there has been a growing trend for the use of activated carbon as a support for the FTS reaction [7,12–16].

In the present study we have investigated the effect of two parameters, namely the heat treatment temperature and the

\* Corresponding author.

E-mail address: [hutch@cardiff.ac.uk](mailto:hutch@cardiff.ac.uk) (G.J. Hutchings).

precipitate ageing time on the catalytic activity of  $\text{CoMnO}_x$  catalysts supported on carbon. Both of these factors have been shown to effect catalytic activity and the product selectivity previously [17,18].

## 2. Experimental

### 2.1. Catalyst preparation

#### 2.1.1. Co-precipitation

$\text{CoMnO}_x$  catalysts were prepared according to the procedure given in the patent literature [16,19]. An aqueous solution was prepared containing equimolar amounts of cobalt nitrate hexahydrate ( $\text{Co}(\text{NO}_3)_2 \cdot 6\text{H}_2\text{O}$ , Sigma-Aldrich, 99.99%) and manganese nitrate tetrahydrate ( $\text{Mn}(\text{NO}_3)_2 \cdot 4\text{H}_2\text{O}$ , Sigma-Aldrich, ≥98%). This solution was heated to 80 °C and aqueous ammonia (28–30%  $\text{NH}_3$  in water, Sigma-Aldrich) was added to raise the pH from 2.9 to  $8.30 \pm 0.01$ . The resulting precipitate was recovered by filtration, washed with distilled water (1 dm<sup>3</sup>, 80 °C), dried (110 °C, 16 h) and calcined in static air (500 °C, 24 h).

#### 2.1.2. Deposition precipitation

$\text{CoMnO}_x/\text{C}$  catalysts were prepared as according to the procedure given in the patent literature [16,19]. An aqueous solution was prepared containing equimolar amounts of cobalt nitrate hexahydrate ( $\text{Co}(\text{NO}_3)_2 \cdot 6\text{H}_2\text{O}$ , Sigma-Aldrich, 99.99%) and manganese nitrate tetrahydrate ( $\text{Mn}(\text{NO}_3)_2 \cdot 4\text{H}_2\text{O}$ , Sigma Aldrich, ≥98%). Coconut shell-derived activated carbon (GCN3070, NORIT) was added to the mixed nitrate solution to give a final catalyst with a composition of 20% Co, 20% Mn and 60% activated carbon. The slurry was stirred for 10 min at 80 °C before aqueous ammonia (28–30%  $\text{NH}_3$  in  $\text{H}_2\text{O}$ , Sigma-Aldrich) was added drop wise to the nitrate solution to raise the pH from 4 to  $8.30 \pm 0.01$ . The resulting precipitate was recovered by filtration, washed with distilled water (1 L, 80 °C), dried (110 °C, 16 h) and heated in flowing He.

To study the effect of heat treatment, one batch of catalyst was divided into four portions which were heated in flowing He separately at 300, 400, 500, and 600 °C for 5 h.

To study the effect of ageing the precipitate was left in the mother liquor for the specific time intervals of 1, 2, and 3 h followed by heat treatment in He at 500 °C for 5 h.

### 2.2. Catalytic activity

The catalysts were pelleted and sieved (0.65–0.85 mm) and 0.5 g were loaded into stainless steel fixed bed reactors (internal diameter 8 mm). Catalysts were reduced *in situ* at 400 °C for 16 h in pure hydrogen ( $\text{GHSV} = 600 \text{ h}^{-1}$ ) then cooled to room temperature and pressurized to 6 bar with syngas ( $\text{CO:H}_2 = 1:1$  molar ratio). All catalysts were tested under identical reaction conditions, 240 °C, 6 bar, and  $\text{GHSV} = 600 \text{ h}^{-1}$ .

A stabilization period of ~100 h was allowed before catalyst data was collected and the mass balance determined. Analysis of gas products was performed by on-line gas chromatography using a Varian GC-3800. Hydrocarbons were analyzed using a CP-Al<sub>2</sub>O<sub>3</sub>/KCl column and a flame ionization detector. Permanent gases and C<sub>1</sub>–C<sub>4</sub> hydrocarbons were analyzed using molecular sieve 13× and Poropak Q columns with TCD and FID detectors in series. Nitrogen was used as an internal standard. The product stream was cooled in a wax trap (~25 °C) to retain the liquid products. Calibrations were performed with standard samples (C<sub>1</sub>–C<sub>5</sub> hydrocarbon mixture diluted with nitrogen, BOC certified) for data quantification.

## 2.3. Catalyst characterization

### 2.3.1. X-ray photoelectron spectroscopy (XPS)

XPS was performed using a Kratos Axis Ultra-DLD photoelectron spectrometer, using monochromatic Al K $\alpha$  radiation, at 144 W. High resolution and survey scans were performed at pass energies of 40 and 160 eV, respectively. Spectra were calibrated to the C (1s) signal at 284.5 eV, which is typical for graphitic carbon as measured for HOPG, and quantified using CasaXPS v2.3.15, utilizing sensitivity factors supplied by the manufacturer.

### 2.3.2. Powder X-ray diffraction (XRD)

XRD measurements were performed using a Bruker AXS Company, D8 Advance diffractometer. Scans were taken with a 2 $\theta$  step size of 0.02° and a counting time of 1.0 s using Cu K $\alpha$  radiation source generated at 40 kV and 30 mA. Specimens for XRD were prepared by compaction into a glass-backed aluminium sample holder. Data was collected over a 2 $\theta$  range from 4° to 80° and phases identified by matching with the ICDD database.

## 3. Results and discussion

### 3.1. Comparison of catalyst performance of $\text{CoMnO}_x$ and $\text{CoMnO}_x/\text{C}$ catalysts

The unaged catalysts were tested for the FTS reaction under identical conditions and the data are presented in Table 1. A comparison of the  $\text{CoMnO}_x$  and  $\text{CoMnO}_x/\text{C}$  catalyst performance indicates the selectivity to carbon dioxide and methane was decreased markedly with the carbon-supported catalyst. CO conversion and the selectivity to C<sub>5+</sub> hydrocarbons were higher compared with the pure  $\text{CoMnO}_x$  catalyst. The effect of time-on-line is presented in Fig. 1 and this shows that the carbon-supported catalyst attained steady state after 45 h, whereas the unsupported  $\text{CoMnO}_x$  catalyst achieved steady state only after 90 h. Neither catalyst showed deactivation over the time period studied.

### 3.2. Effect of preparation variables on the performance of $\text{CoMnO}_x/\text{C}$ catalysts

#### 3.2.1. Pre-treatment temperature

Pretreatment of the catalyst precursor, particularly the heat treatment temperature is a critical parameter in catalyst preparation which can affect the activity and selectivity of the catalysts [17]. In order to study the effect of the pretreatment, one batch of  $\text{CoMnO}_x/\text{C}$  was heated at different temperatures in He. Intervals of 100 °C were selected and although relatively large they are considered to be appropriate for this initial screening study. CO conversion and product selectivity data are presented in Table 2 and it is apparent that there was a steady increase in CO conversion with increasing heat treatment temperatures from 300 to 500 °C. An

**Table 1**

Comparison of the catalytic activity of  $\text{CoMnO}_x$  with  $\text{CoMnO}_x/\text{C}$  catalyst.

	$\text{CoMnO}_x$	$\text{CoMnO}_x/\text{C}$
CO conversion (%)	36.0	48
Product selectivity (%)		
CH <sub>4</sub>	22.1	7.0
C <sub>2</sub>	4.5	4.3
C <sub>3</sub>	11.5	16.1
C <sub>4</sub>	1.2	7.6
C <sub>5+</sub>	17.0	43.4
CO <sub>2</sub>	37.0	20.4
Alcohols	6.7	2.2

Reaction conditions: Catalyst 0.5 g, data collected at 135 h, 240 °C, 6 bar, CO:H<sub>2</sub> 1:1 mol ratio, GHSV 600 h<sup>-1</sup>.

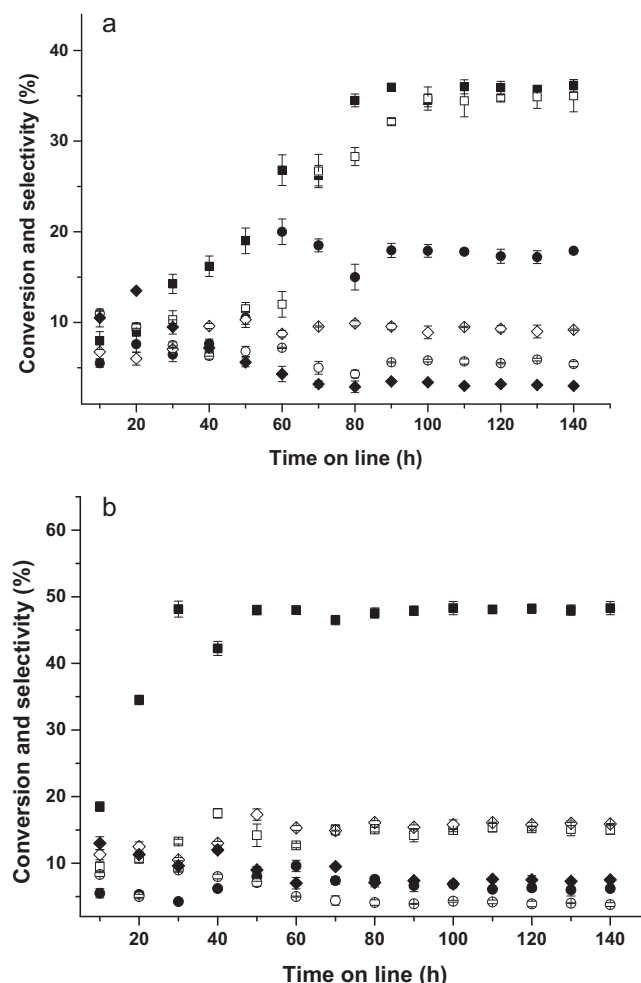


**Fig. 1.** Time on line study on (a)  $\text{CoMnO}_x$  catalyst, (b)  $\text{CoMnO}_x/\text{C}$  catalyst. ■ CO conversion, □  $\text{CO}_2$ , ●  $\text{CH}_4$ , ○  $\text{C}_2$ , ◇  $\text{C}_3$ , ♦  $\text{C}_4$ . Error bars are shown, if not visible the error is equivalent in scale to the symbol.

increase in  $\text{C}_{5+}$  product selectivity was also observed together with a decrease in  $\text{CO}_2$  selectivity. Previously, heat treatment studies of this type have been performed for oxide-supported Co catalysts [18], but to date this has not been carried out for carbon-supported  $\text{CoMnO}_x$  catalysts.

For the catalyst pretreated at  $600^\circ\text{C}$  the CO conversion and the selectivity to  $\text{CH}_4$  and  $\text{CO}_2$  decreased markedly together with an increase in the selectivity of  $\text{C}_{5+}$  products. This corresponds to a structural change which is evident from the XRD patterns (Fig. 2). All catalysts showed the diffraction pattern for the mixed spinel oxide of Co and Mn (with an intermediate tetragonal structure

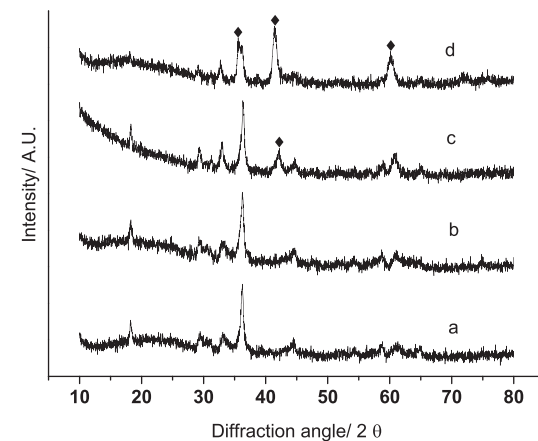


**Fig. 2.** Powder X-ray diffraction pattern for  $\text{Co}/\text{Mn}/\text{C}$  catalysts heated at different temperatures: (a)  $300^\circ\text{C}$ , (b)  $400^\circ\text{C}$ , (c)  $500^\circ\text{C}$ , (d)  $600^\circ\text{C}$ . ♦ Co.

**Table 3**

Effect of heat treatment on the particle size of the  $\text{CoMn}_2\text{O}_4$  phase.

Heat treatment temperature ( $^\circ\text{C}$ )	Particle size (nm)
300	8.8
400	9.2
500	9.4
600	11.2

between  $\text{CoMn}_2\text{O}_4$  and  $\text{Mn}_3\text{O}_4$ ) (ICDD 018-0408). The XRD pattern of the catalysts heated at  $300$  and  $400^\circ\text{C}$  were found to be similar to each other, whilst an additional phase of Co metal was observed with a reflection at  $41.9^\circ$  (ICDD 15-0806) in the catalyst pretreated at  $500^\circ\text{C}$  in addition to the mixed spinel oxide phases of  $\text{CoMn}_2\text{O}_4$ . The catalyst treated at  $600^\circ\text{C}$  displays the most significant change in the XRD pattern, with Co reflections at  $36.0^\circ$ ,  $41.9^\circ$  and  $60.1^\circ$   $2\theta$  (ICDD 15-0806). This indicates that the Co nanoparticles are sintering and hence here is a loss in activity. Particle sizes of the  $\text{CoMn}_2\text{O}_4$  phase were calculated using the Scherrer equation and the data are presented in Table 3 and it is apparent that the particle size only increases markedly for the catalyst heated at  $600^\circ\text{C}$ .

XPS derived molar concentrations are given in Table 4 and it is evident that there was no significant change in the Co:Mn molar ratios for heat treatments up to  $500^\circ\text{C}$ , whereas the surface becomes Mn rich above this temperature. XPS core-level spectra in Fig. 3 show that with increasing treatment temperature the main  $\text{Co}(2p_{3/2})$  photoelectron signal remains consistent with  $\text{Co}^{2+}$  (ca.  $780\text{ eV}$ ). However, concomitant with increasing heating temperature is the development of the shake-up satellite structure above the main  $\text{Co}(2p_{3/2})$  photoemission line (indicated by an arrow in Fig. 3a) with the shape and intensity typical for high spin Co (II) [20] and this is consistent with the transformation of  $\text{CoMn}_2\text{O}_4$  to  $\text{CoO}$  in the precursor.

Changes in the Mn spectra are more subtle, with a shift downward in binding energy of  $0.5\text{ eV}$  between the samples prepared using heat treatment in He at  $300$  ( $641.9\text{ eV}$ ) and  $600^\circ\text{C}$  ( $641.4\text{ eV}$ ). For the catalyst heated at  $600^\circ\text{C}$  the Mn ( $2p_{3/2}$ ) peak reveals some

**Table 2**

Effect of heat treatment during preparation of  $\text{CoMnO}_x/\text{C}$  catalysts.

Heat treatment temperature ( $^\circ\text{C}$ )	300	400	500	600
CO conversion (%)	41.2	47.0	48.9	18.1
Product selectivity (%)				
$\text{CH}_4$	15.1	16.9	8.4	1.3
$\text{C}_2$	8.3	5.3	5.6	1.7
$\text{C}_3$	23.2	20	17.1	6.3
$\text{C}_4$	3.2	3.6	7.0	1.1
$\text{C}_{5+}$	22.7	26.3	41.4	89.6
$\text{CO}_2$	13.5	15.1	19.4	0
Alcohols	14.1	12.8	1.2	0

Reaction conditions: Catalyst 0.5 g,  $240^\circ\text{C}$ , data collected at  $146\text{ h}$ , 6 bar,  $\text{CO:H}_2$  1:1 mol ratio, GHSV  $600\text{ h}^{-1}$ .

**Table 4**

XPS derived molar concentrations for each preparation temperature.

Heat treatment temperature ( $^\circ\text{C}$ )	Molar composition (%)				Ratios
	O	C	Co	Mn	
300	38.7	36.5	12.4	12.5	1.01
400	43.5	27.7	15.0	13.8	0.92
500	43.3	27.8	14.1	14.8	1.05
600	39.5	34.7	8.1	17.7	2.19

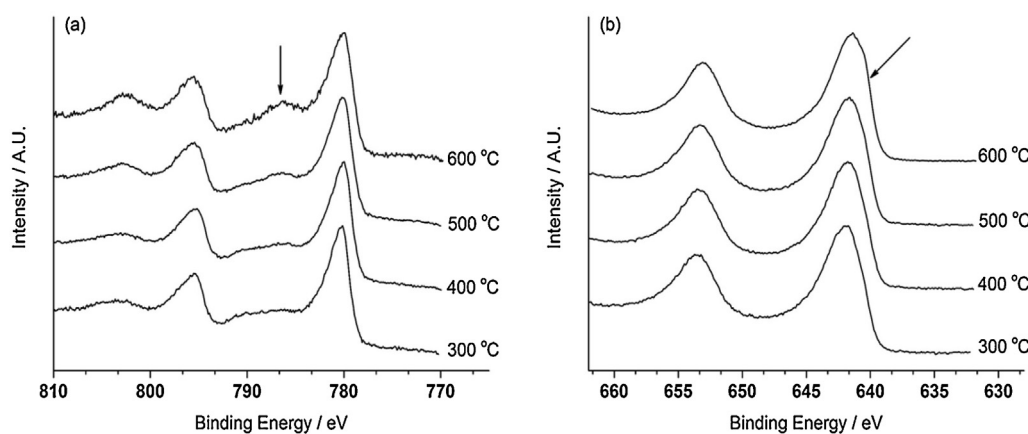


**Fig. 3.** X-ray photoelectron core-level spectra for Co/Mn/C catalysts treated at different temperatures: (a) Co(2p) and (b) Mn(2p).

asymmetry to the lower binding energy side of the peak (indicated by an arrow, Fig. 3b) suggesting the formation of MnO at the surface. XRD data (Fig. 2) indicates that both  $\text{CoMn}_2\text{O}_4$  and Co are present in the precursor for the sample heated at 600 °C, however, XPS analysis of the Co(2p) regions indicates the presence of CoO, which is attributed to Co being oxidized by exposure to air prior to analysis. This also explains the surface enrichment of Mn, and although CoO is also present at the surface, larger particles of CoO would give a lower apparent surface concentration. Clearly from the XRD and XPS analysis, the surface of this catalyst is different than the bulk. However, there is no  $\text{MnO}_x$  phases observed in the XRD pattern, which suggests that any  $\text{MnO}_x$  phases present are poorly crystalline.

### 3.2.2. Ageing time of the precipitates

Having explored the pretreatment temperature of the precursor, we next studied the influence of the ageing time of the precipitate during the catalyst preparation. Ageing of precipitates for different time intervals has been found to be an important parameter in catalyst preparation [21]. Catalysts were prepared with a range of ageing times and then heated in He at 500 °C as this was observed to be the optimum treatment temperature. The activity data is provided in Table 5 and shows that the unaged catalyst exhibits lower selectivity to carbon dioxide and methane. Interestingly, there is a steady decrease in CO conversion and selectivity to  $\text{C}_{5+}$  hydrocarbons with an increase in ageing time of the precipitate.  $\text{CO}_2$  selectivity also increased but the selectivity to  $\text{CH}_4$  remained unchanged.

Previous studies on the effect of ageing time on cobalt oxide catalysts for various gas phase reactions [17,21] have reported that the ageing of precipitates prepared by co-precipitation leads to phase changes towards thermodynamically stable materials. The phase

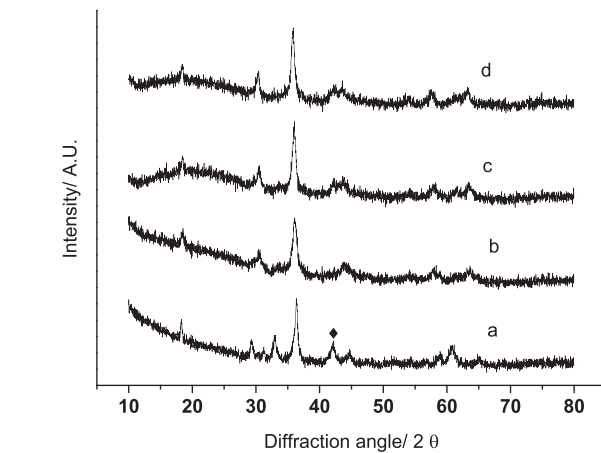


**Fig. 4.** Powder X-ray diffraction pattern for Co/Mn/C catalysts prepared with different ageing times of: (a) unaged, (b) 1 h, (c) 2 h and (d) 3 h. ♦ Co.

analysis of the aged catalysts has been investigated by XRD and the data are shown in Fig. 4. All materials exhibit the pattern for the mixed spinel oxide of Co and Mn with an intermediate tetragonal structure between  $\text{CoMn}_2\text{O}_4$  and  $\text{Mn}_3\text{O}_4$  (ICDD 018-0408). A Co phase was evident in the unaged catalyst from the reflection at 41.9° 2θ (ICDD 15-0806), but increased ageing times led to the formation of the cubic  $\text{CoMn}_2\text{O}_4$  phase (ICDD 023-1237) and the Co was no longer apparent. Particle sizes for the  $\text{CoMn}_2\text{O}_4$  phase were calculated using the Scherrer equation and the data are provided in Table 6 and an increase in the particle size is observed with an increase in the ageing time of the precipitate.

The XPS derived molar ratios or Co and Mn analysis are given in Table 7, whilst Fig. 5 shows Co(2p) and Mn(2p) core-level spectra. For the unaged sample, the  $\text{Co}(2p_{3/2})$  peak at 780.2 eV is indicative of  $\text{Co}^{2+}$ , with an associated satellite structure at higher binding energy confirming the XRD evidence that CoO is present. The  $\text{Mn}(2p_{3/2})$  peak energy of 641.3 eV can be assigned to  $\text{Mn}_x\text{O}_y$  or  $\text{CoMn}_2\text{O}_4$  and again this is in agreement with the XRD data. With increased ageing time, both Co and Mn binding energies shift to slightly higher binding energy, consistent with the bulk  $\text{CoMn}_2\text{O}_4$ .

**Table 5**

Effect of ageing time of the precipitate on the activity and selectivity of  $\text{CoMnO}_x/\text{C}$  catalysts.

	0 h	1 h	2 h	3 h
CO conversion (%)	48.9	36.8	29.6	27
Product selectivity (%)				
CH <sub>4</sub>	8.4	8.3	8.9	9.2
C <sub>2</sub>	5.6	4.4	4.8	6.0
C <sub>3</sub>	17.1	17.5	14.5	16.7
C <sub>4</sub>	7.0	5.1	5.6	5.7
C <sub>5+</sub>	41.4	40.0	35.0	25.0
CO <sub>2</sub>	19.4	23.0	29.0	38.0
Alcohols	1.2	2.0	3.0	0.0

Reaction conditions: catalyst 0.5 g, 240 °C, data collected at 140 h, 6 bar, CO:H<sub>2</sub> 1:1 mol ratio, GHSV 600 h<sup>-1</sup>.

**Table 6**

Effect of the precipitate ageing time on the particle size of the  $\text{CoMn}_2\text{O}_4$  phase.

Ageing time (h)	Particle size (nm)
0	9.3
1	9.6
2	10.1
3	10.4

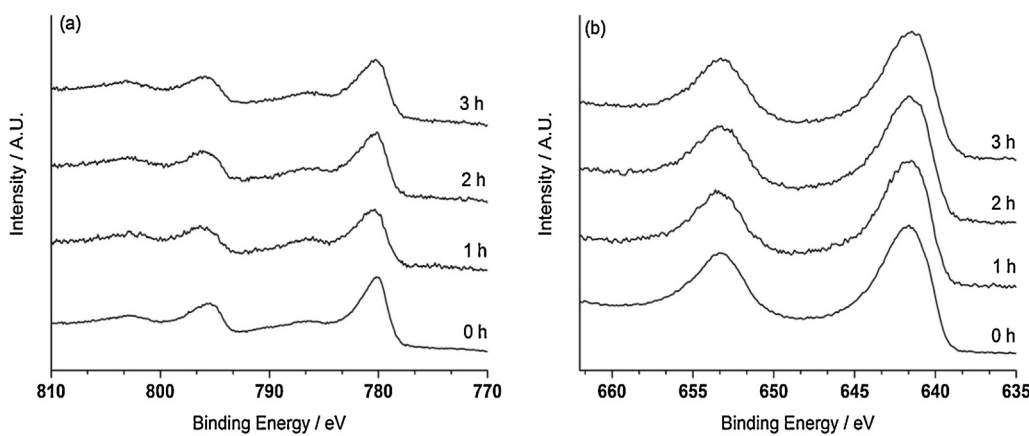


**Fig. 5.** X-ray photoelectron core-level spectra for Co/Mn/C catalysts with different ageing times: (a) Co(2p) and (b) Mn(2p).

**Table 7**  
XPS derived molar surface concentrations for Co/Mo/C aged for different times.

Ageing time (h)	Molar composition (%)				Ratio
	O	C	Co	Mn	
0	43.3	27.8	14.1	14.8	1.05
1	15.6	76.9	3.0	4.4	1.45
2	18.8	69.3	5.6	6.4	1.15
3	22.8	61.7	7.1	8.5	1.20

[22]. There is an increase in amount of both metals on the surface of these catalysts with an increase in ageing time.

The Mn:Co molar ratios clearly show that the unaged catalyst exhibits a metal ratio close to unity as expected from the catalyst preparation, however, longer ageing times initially seem to decrease the apparent surface metal content, with a subsequent increase at higher ageing times which can be linked to the initial uptake of the metals in to the porous network of the carbon followed by further accumulation at the surface.

#### 4. Conclusions

We have investigated and contrasted carbon-supported cobalt manganese oxide ( $\text{CoMnO}_x/\text{C}$ ) catalysts and an unsupported  $\text{CoMnO}_x$  catalyst for the FTS reaction. The carbon-supported catalyst gave increased catalyst activity and selectivity to  $\text{C}_{5+}$  hydrocarbons and the selectivity to  $\text{CH}_4$  and  $\text{CO}_2$  was decreased in comparison to the  $\text{CoMnO}_x$  catalyst. In addition the carbon-supported catalysts attained a steady state performance far more rapidly than the unsupported catalyst. The effect of two key parameters; namely the heat treatment of the precursor prior to reduction and the effect of ageing of the initial precipitate have been studied and the optimal conditions identified. Most importantly ageing of the initial precipitate and high temperature treatment of the precursor should be avoided to obtain an effective catalyst performance.

#### Acknowledgement

We are thankful to SABIC for financial support.

#### References

- [1] R.G. Copperthwaite, G.J. Hutchings, M. Van der Riet, J. Woodhouse, Ind. Eng. Chem. Res. 26 (1987) 869–874.
- [2] M. Van der Riet, G.J. Hutchings, R.G. Copperthwaite, J. Chem. Soc. Chem. Commun. (1986) 798–799.
- [3] M. Arsalanfar, A.A. Mirzaei, H. Atashi, H.R. Bozorgzadeh, S. Vahid, A. Zare, Fuel Process. Technol. 96 (2012) 150–159.
- [4] A.P. Hindermann, G.J. Hutchings, A. Kiennemann, Catal. Rev. Sci. Eng. 35 (1993) 19–35.
- [5] A.Y. Khodakov, W. Chu, P. Fongaland, Chem. Rev. 107 (2007) 1692–1744.
- [6] G.R. Johnson, S. Werner, K.C. Bustillo, P. Ercius, C. Kisielowski, A.T. Bell, J. Catal. 328 (2015) 111–122.
- [7] N.E. Tsakoumis, M. Ronning, O. Borg, E. Rytter, A. Holmen, Catal. Today 154 (2010) 162–182.
- [8] G.L. Bezemer, P.B. Radstake, U. Falke, H. Oosterbeek, H.P.C.E. Kuipers, A.J. van Dillen, K.P. de Jong, J. Catal. 237 (2006) 152–161.
- [9] G.V. Pankina, P.A. Chernavskii, V.O. Kazak, V.V. Lunin, J. Phys. Chem. A 89 (2015) 1065–1069.
- [10] K.-S. Ha, G. Kwak, K.-W. Jun, J. Hwang, J. Lee, Chem. Commun. 49 (2013) 5141–5143.
- [11] H. Xiong, M. Moyo, M.K. Rayner, L.L. Jewell, D.G. Billing, N.J. Coville, ChemCatChem 2 (2010) 514–518.
- [12] A. Dinse, M. Aigner, M. Ulbrich, G.R. Johnson, A.T. Bell, J. Catal. 288 (2012) 104–114.
- [13] R.D. Oades, S.R. Morris, R.B. Moyes, Catal. Today 7 (1990) 199–208.
- [14] H. Ban, Z. Wang, Z. Wang, Z. Fang, Adv. Mater. Res. 805–806 (2013) 232–235.
- [15] J.M. Solar, F.J. Derbyshire, V.H.J. De Beer, L.R. Radovic, J. Catal. 129 (1991) 330–342.
- [16] K. Karim, G. Hutchings, S. Iqbal, WO2012143131A1, 2012.
- [17] B. Solsona, G.J. Hutchings, T. Garcia, S.H. Taylor, New J. Chem. 28 (2004) 708–711.
- [18] M. Feyzi, M.M. Khodaei, J. Shahmoradi, Fuel Process. Technol. 93 (2012) 90–98.
- [19] K. Karim, S. Al-sayaria, G.J. Hutchings, S. Iqbal, WO2014174374, 2014.
- [20] H.T. Zhang, X.H. Chen, Nanotechnology 17 (2006) 1384–1390.
- [21] A.A. Mirzaei, M. Faizi, R. Habibpour, Appl. Catal. A 306 (2006) 98–107.
- [22] M. Oku, K. Hirokawa, J. Electron Spectrosc. Relat. Phenom. 8 (1976) 475–481.